ELSEVIER

International Journal of Solids and Structures 41 (2004) 2757–2779

INTERNATIONAL JOURNAL OF SOLIDS and STRUCTURES

www.elsevier.com/locate/ijsolstr

On the energy release rate and mode mix of delaminated shear deformable composite plates

Jialai Wang, Pizhong Qiao *

Department of Civil Engineering, The University of Akron, Auburn Science and Engineering Center, 244 Sumner Street, Akron, OH 44325-3905, USA

Received 3 January 2003; received in revised form 21 October 2003

Abstract

A first-order shear deformable plate theory-based method is developed to calculate the strain energy release rate and stress intensity factor of a non-homogeneous delaminated composite plate under a general three-dimensional (3-D) loading condition. By modeling the delaminated plate as two shear deformable sub-laminates on either side of the delaminated plane, the strain energy release rate is expressed in terms of three concentrated forces at the crack tip and their corresponding compliance coefficients. The simple expression of strain energy release rate makes the mode decomposition under complicated loading situation possible with the aid of two supplementary continuum analyses. To illustrate the present method, a plain strain delamination problem of laminates is examined, and the closed-form expressions of strain energy release rate and stress intensity factor are obtained. It is found that the available solutions, such as the ones based on the classical plate theory, can be recovered from the present solutions by simply neglecting the transverse shear force. The relationship between the global and local decompositions is further established, and the accuracy of the present solutions is examined by comparing with numerical results of boundary element method. With inclusion of transverse shear deformation in the formulation, more accurate and explicit predictions of the strain energy release rate and stress intensity factor of delaminated composite plate are achieved by the present method, especially when a laminate has a relatively low transverse shear modulus or moderate thickness.

Keywords: Laminated composites; Delamination; Shear deformable plates; Crack tip; Mode decomposition; Transverse shear deformation

1. Introduction

Interlaminar delamination is one of most common failure modes in composites laminates. Fracture mechanics principles have been widely employed to assess this type of failure mode, where the strain energy

* Corresponding author. Tel.: +1-330-972-5226; fax: +1-330-972-6020.
E-mail address: qiao@uakron.edu (P. Qiao).

0020-7683/$ - see front matter © 2003 Elsevier Ltd. All rights reserved.
doi:10.1016/j.ijsolstr.2003.11.039

release rate (SERR) G or stress intensity factor (SIF) K is evaluated and compared with the critical mode-mix-dependent SERR G_c or SIF K_c of the interface determined from experiments. The interface crack is likely to propagate if G or K reaches G_c or K_c. This approach was adopted by Wang and Crossman (1980), Wang (1982), O'Brien (1982, 1990), and Davidson et al. (2000a). By noting the mode mix dependence of G_c and K_c, it is often necessary to extract the mode mix of G and K at the crack tip in order to successfully predict the growth of crack.

Extensive studies have been conducted on predictions of both the SERR and SIF of elastic layered structures (Suo and Hutchinson, 1990; Schapery and Davidson, 1990; Davidson et al., 1995; Sheinman and Kardomateas, 1997). Finite elements have been frequently used to calculate the SIF (K) or SERR (G) and mode mix of the interface crack for general conditions (Matos et al., 1989; Venkatesha et al., 1996; Beuth, 1996; Sun and Qian, 1997; Qian and Sun, 1998; Nillsson et al., 2001). When the beam/plate-type layered structures are encountered, however, the application of finite elements is not efficient since the K-dominant zone is relatively small, and very fine mesh near the crack tip is required to obtain sufficiently accurate results. In such a case, a more efficient alternative is to take the advantage of lamination plate theory to calculate the SERR and obtain the SIF by solving supplemental continuum problem. This method is remarkably simple, and therefore, computationally efficient, as proposed and illustrated by Schapery and Davidson (1990) and Suo and Hutchinson (1990). In the classical works of Schapery and Davidson (1990), Suo and Hutchinson (1990), and Davidson et al. (1995), the SERR of an interface crack between two elastic layers was calculated by a classical beam or plate theory and expressed in terms of two independent loading parameters P and M (Suo and Hutchinson, 1990) or concentrated force and moment at the crack tip (Schapery and Davidson, 1990); but the mode mix was retrieved through an auxiliary continuum analysis. This method, commonly known as crack tip element (CTE) analysis (Davidson et al., 1995), was successfully used in the interface fracture analysis in two-dimensional (2-D) situation (Davidson and Sundararaman, 1996). However, the shear deformation in the cracked and uncracked regions is not considered in the existing models since the classical beam or plate theory was basically used. As a result, the SERR is always underestimated by this method (Davidson and Sundararaman, 1996). This limitation is also demonstrated in the studies to extend the 2-D CTE to 3-D situation where the out-of-plane shear force is included (Hu, 1995; Yang et al., 2000). Davidson et al. (2000b) found that the total and out-of-plane shear SERRs calculated by the classical plate theory based 3-D CTE is erroneous. As a modification, they introduced shear deformation kinematics to calculate plate forces and moments near the delamination tip and then substituted the resulting loading parameters into the CTE model to calculate the SERR. By this way, the errors due to shear deformation were reduced, and a good agreement with the predictions by 3-D finite element analysis was reached. However, the inconsistence between the SERR predictions based on the shear deformable and classical plate theory was introduced in their model. Sanker and co-workers (Sankar and Sonik, 1995; Park and Sanker, 2002) took a similar approach to obtain the SERR; the first-order shear deformation theory was used in their model, and the point-wise SERR was expressed in terms of jumps of three forces and two moments across the delamination front. Although the transverse shear deformation was included in the formulation, the expression of the SERR is relatively complicated, and it is difficult to retrieve the mode mix.

In this study, we aim to establish a simple method to calculate the SERR and SIF of a delamination in the shear deformable composite laminates. The formulation incorporates the shear deformation of laminates and can be used to predict the delamination in the laminated composites. An explicit and more accurate expression of the SERR is obtained first by using the first-order shear deformation laminate theory. Then a method to decompose the mode mix of SIF is proposed. To illustrate the present method, a plain strain delamination problem is studied, and a closed-form solution of the SERR and SIF is obtained. The explicit solution obtained in this study is then compared with the available classical solutions in the literature and with the numerical results of boundary element method.

2. Strain energy release rate under general loading conditions

Consider a small piece at the delamination tip of Fig. 1, where a delamination s lies along the straight interface of the top plate "1" and bottom plate "2" with thickness of h_1 and h_2, respectively. Generic loads are applied, as already determined by a global beam or plate analysis.

In the conventional CTE analysis (Davidson et al., 1995; Yang et al., 2000), this problem is modeled as three classical plates: the top plate in the cracked region, the bottom plate in the cracked region, and a single plate of the whole uncracked region. As shown in Bruno and Greco (2001), it is not appropriate to model the undelaminated portion of the laminate using a single plate element in which the actual shear deformation could not be captured. Therefore, in this study, the uncracked region is modeled as two plates as the ones in the cracked region: top plate "1" and bottom plate "2", instead of only one single plate. These two plates are perfectly bonded along their interface to keep the continuity of displacement; while the two plates in cracked region deform separately. The first-order shear deformation theory or Reissner–Mindlin plate theory is used in this study to account for the shear deformation, and the top and bottom plates can be in laminate configuration (i.e., sub-laminates 1 and 2, respectively).

2.1. First-order shear deformation theory of laminate plate

According to Reissner–Mindlin plate theory, the deformations of a two-plate system are given as:

$$U_i(x,y,z) = u_i(x,y) + z\phi_{xi}(x,y) \tag{1}$$

$$V_i(x,y,z) = v_i(x,y) + z\phi_{yi}(x,y) \tag{2}$$

$$W_i(x,y,z) = w_i(x,y) \tag{3}$$

where the subscript $i = 1$ or 2, represents the plate 1 or 2 in Fig. 1, respectively.

The strains in these two plates are given as:

$$\begin{aligned}
&\varepsilon_{xxi} = \varepsilon^0_{xxi} + z\kappa_{xi}, \quad \varepsilon^0_{xxi} = \frac{\partial u_i}{\partial x}, \quad \kappa_{xi} = \frac{\partial \phi_{xi}}{\partial x} \\
&\varepsilon_{yyi} = \varepsilon^0_{yyi} + z\kappa_{yi}, \quad \varepsilon^0_{yyi} = \frac{\partial v_i}{\partial y}, \quad \kappa_{yi} = \frac{\partial \phi_{yi}}{\partial y} \\
&\gamma_{xyi} = \gamma^0_{xyi} + z\kappa_{xyi}, \quad \gamma^0_{xyi} = \frac{\partial v_i}{\partial x} + \frac{\partial u_i}{\partial y}, \quad \kappa_{xyi} = \frac{\partial \phi_{yi}}{\partial x} + \frac{\partial \phi_{xi}}{\partial y} \\
&\gamma_{xzi} = \gamma^0_{xzi} = \phi_{xi} + \frac{\partial w_i}{\partial x}, \quad \gamma_{yzi} = \gamma^0_{yzi} = \phi_{yi} + \frac{\partial w_i}{\partial y}
\end{aligned} \tag{4}$$

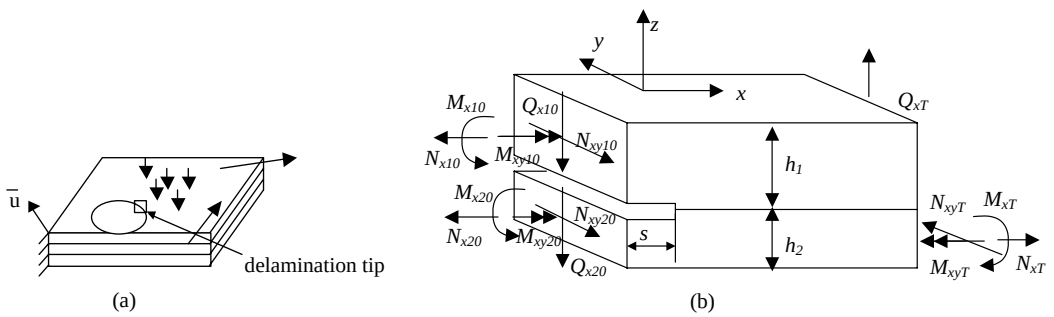

Fig. 1. Delamination in composite laminate. (a) A laminated plate under general loadings and (b) element at the delamination tip.

The constitutive equation of a laminated plate is written in the conventional way (Barbero, 1998) as:

$$\begin{pmatrix} N_{xi} \\ N_{yi} \\ N_{xyi} \\ M_{xi} \\ M_{yi} \\ M_{xyi} \end{pmatrix} = \begin{pmatrix} A_{11}^{(i)} & A_{12}^{(i)} & A_{16}^{(i)} & B_{11}^{(i)} & B_{12}^{(i)} & B_{16}^{(i)} \\ A_{12}^{(i)} & A_{22}^{(i)} & A_{26}^{(i)} & B_{12}^{(i)} & B_{22}^{(i)} & B_{26}^{(i)} \\ A_{16}^{(i)} & A_{26}^{(i)} & A_{66}^{(i)} & B_{16}^{(i)} & B_{26}^{(i)} & B_{66}^{(i)} \\ B_{11}^{(i)} & B_{12}^{(i)} & B_{16}^{(i)} & D_{11}^{(i)} & D_{12}^{(i)} & D_{16}^{(i)} \\ B_{12}^{(i)} & B_{22}^{(i)} & B_{26}^{(i)} & D_{12}^{(i)} & D_{22}^{(i)} & D_{26}^{(i)} \\ B_{16}^{(i)} & B_{26}^{(i)} & B_{66}^{(i)} & D_{16}^{(i)} & D_{26}^{(i)} & D_{66}^{(i)} \end{pmatrix} \begin{pmatrix} \varepsilon_{xxi}^{0} \\ \varepsilon_{yyi}^{0} \\ \gamma_{xyi}^{0} \\ \kappa_{xi} \\ \kappa_{yi} \\ \kappa_{xyi} \end{pmatrix}$$

$$\begin{pmatrix} Q_{yi} \\ Q_{xi} \end{pmatrix} = \begin{pmatrix} A_{44}^{(i)} & A_{45}^{(i)} \\ A_{45}^{(i)} & A_{55}^{(i)} \end{pmatrix} \begin{pmatrix} \gamma_{yzi} \\ \gamma_{xzi} \end{pmatrix} \tag{5}$$

or,

$$\begin{pmatrix} \frac{\partial u_i}{\partial x} \\ \frac{\partial v_i}{\partial y} \\ \frac{\partial v_i}{\partial x} + \frac{\partial u_i}{\partial y} \\ \frac{\partial \phi_{xi}}{\partial x} \\ \frac{\partial \phi_{yi}}{\partial y} \\ \frac{\partial \phi_{yi}}{\partial x} + \frac{\partial \phi_{xi}}{\partial y} \end{pmatrix} = \begin{pmatrix} a_{11}^{(i)} & a_{12}^{(i)} & a_{16}^{(i)} & b_{11}^{(i)} & b_{12}^{(i)} & b_{16}^{(i)} \\ a_{12}^{(i)} & a_{22}^{(i)} & a_{26}^{(i)} & b_{12}^{(i)} & b_{22}^{(i)} & b_{26}^{(i)} \\ a_{16}^{(i)} & a_{26}^{(i)} & a_{66}^{(i)} & b_{16}^{(i)} & b_{26}^{(i)} & b_{66}^{(i)} \\ b_{11}^{(i)} & b_{12}^{(i)} & b_{16}^{(i)} & d_{11}^{(i)} & d_{12}^{(i)} & d_{16}^{(i)} \\ b_{12}^{(i)} & b_{22}^{(i)} & b_{26}^{(i)} & d_{12}^{(i)} & d_{22}^{(i)} & d_{26}^{(i)} \\ b_{16}^{(i)} & b_{26}^{(i)} & b_{66}^{(i)} & d_{16}^{(i)} & d_{26}^{(i)} & d_{66}^{(i)} \end{pmatrix} \begin{pmatrix} N_{xi} \\ N_{yi} \\ N_{xyi} \\ M_{xi} \\ M_{yi} \\ M_{xyi} \end{pmatrix}$$

$$\begin{pmatrix} \phi_{yi} + \frac{\partial w_i}{\partial y} \\ \phi_{xi} + \frac{\partial w_i}{\partial x} \end{pmatrix} = \begin{pmatrix} a_{44}^{(i)} & a_{45}^{(i)} \\ a_{45}^{(i)} & a_{55}^{(i)} \end{pmatrix} \begin{pmatrix} Q_{yi} \\ Q_{xi} \end{pmatrix} \tag{6}$$

The global equilibrium conditions are simply given as (see Figs. 1(b) and 2):

$$N_{x10} + N_{x20} = N_{x1} + N_{x2} = N_{xT}, \qquad N_{y10} + N_{y20} = N_{y1} + N_{y2} = N_{yT} \tag{7}$$

$$Q_{x10} + Q_{x20} = Q_{x1} + Q_{x2} = Q_{xT}, \qquad Q_{y10} + Q_{y20} = Q_{y1} + Q_{y2} = Q_{yT} \tag{8}$$

$$M_{x10} + M_{x20} + N_{x10}\frac{h_1 + h_2}{2} + Q_{xT}x = M_{x1} + M_{x2} + N_{x1}\frac{h_1 + h_2}{2} = M_{xT} \tag{9}$$

$$M_{xy10} + M_{xy20} + N_{xy10}\frac{h_1 + h_2}{2} = M_{xy1} + M_{xy2} + N_{xy1}\frac{h_1 + h_2}{2} = M_{xyT} \tag{10}$$

It has been shown that three concentrated crack tip forces (i.e., N_{xc}, Q_{xc}, and N_{xyc}) coexisting at the crack tip (Chatterjee and Ramnath, 1988) are resulted from the stress singularity at the delaminating tip (Fig. 2). Then the equilibrium equations at the crack tip can be written as:

$$N_{x10} = -N_{xc} + N_{x1}|_{x=0} \tag{11}$$

$$N_{xy10} = -N_{xyc} + N_{xy1}|_{x=0} \tag{12}$$

$$Q_{x10} = -Q_{xc} + Q_{x1}|_{x=0} \tag{13}$$

$$M_{x10} = \frac{h_1}{2}N_{xc} + M_{x1}|_{x=0} \tag{14}$$

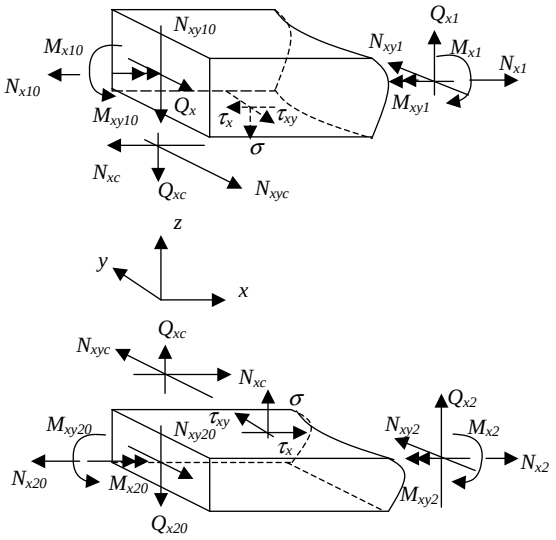

Fig. 2. Stresses and forces at crack tip.

$$M_{xy10} = \frac{h_1}{2} N_{xyc} + M_{xy1}|_{x=0} \tag{15}$$

while N_{yi}, M_{yi} and Q_{yi} are continuous at the crack tip (Sankar and Sonik, 1995).

As a result, the deformations at the crack tip are continuous; however, their gradients are not continuous.

2.2. Determination of SERRs

According to Irwin method (Fig. 3), the strain energy release rates (SERRs) at the crack tip can be computed as:

$$G_{\mathrm{I}} = \lim_{\Delta \to 0} \frac{1}{2\Delta} \int_0^{\Delta} \sigma_z(x)\delta w(\Delta - x)\,\mathrm{d}x = \lim_{\Delta \to 0} \frac{1}{2\Delta} \sigma_z(\zeta)(\delta w(0) - \delta w'(0)\zeta)\Delta \tag{16}$$

$$G_{\mathrm{II}} = \lim_{\Delta \to 0} \frac{1}{2\Delta} \int_0^{\Delta} \tau_x(x)\delta u(\Delta - x)\,\mathrm{d}x = \lim_{\Delta \to 0} \frac{1}{2\Delta} \tau_x(\zeta)(\delta u(0) - \delta u'(0)\zeta)\Delta \tag{17}$$

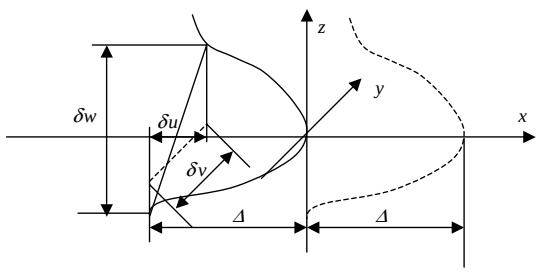

Fig. 3. Calculation of the strain energy release rate by Irwin method.

$$G_{\mathrm{III}} = \lim_{\Delta\to 0}\frac{1}{2\Delta}\int_0^{\Delta}\tau_{xy}(x)\delta v(\Delta - x)\,\mathrm{d}x = \lim_{\Delta\to 0}\frac{1}{2\Delta}\tau_{xy}(\zeta)(\delta v(0) - \delta v'(0)\zeta)\Delta \tag{18}$$

where Δ is a virtual crack propagation length; $\sigma_x(x)$, $\tau_x(x)$ and $\tau_{xy}(x)$ are the surface tractions; x and ζ are the distances from the crack edge (Fig. 3); and $0 < \zeta < \Delta$. Be aware that:

$$\delta u(0) = 0, \qquad \delta v(0) = 0, \qquad \delta w(0) = 0$$

Eqs. (16)–(18) can be rewritten as:

$$G_{\mathrm{I}} = \frac{1}{2}Q_{xc}\frac{\partial(w_1 - w_2)}{\partial x}\bigg|_{x=0-} \tag{19}$$

$$G_{\mathrm{II}} = \frac{1}{2}N_{xc}\frac{\partial\left(u_1 - \frac{h_1}{2}\phi_{x1} - u_2 - \frac{h_2}{2}\phi_{x2}\right)}{\partial x}\bigg|_{x=0-} \tag{20}$$

$$G_{\mathrm{III}} = \frac{1}{2}N_{xyc}\frac{\partial\left(v_1 - \frac{h_1}{2}\phi_{y1} - v_2 - \frac{h_2}{2}\phi_{y2}\right)}{\partial x}\bigg|_{x=0-} \tag{21}$$

At the uncracked part of the laminate ($x \geqslant 0$), the displacement continuity along the interface of two sub-laminates requires:

$$u_1 - \frac{h_1}{2}\phi_{x1} = u_2 + \frac{h_2}{2}\phi_{x2} \tag{22}$$

$$v_1 - \frac{h_1}{2}\phi_{y1} = v_2 + \frac{h_2}{2}\phi_{y2} \tag{23}$$

$$w_1 = w_2 \tag{24}$$

Therefore,

$$\frac{\partial\left(u_1 - \frac{h_1}{2}\phi_{x1} - u_2 - \frac{h_2}{2}\phi_{x2}\right)}{\partial x}\bigg|_{x=0-} = \frac{\partial\left(u_1 - \frac{h_1}{2}\phi_{x1} - u_2 - \frac{h_2}{2}\phi_{x2}\right)}{\partial x}\bigg|_{x=0-} - \frac{\partial\left(u_1 - \frac{h_1}{2}\phi_{x1} - u_2 - \frac{h_2}{2}\phi_{x2}\right)}{\partial x}\bigg|_{x=0+} \tag{25}$$

$$\frac{\partial\left(v_1 - \frac{h_1}{2}\phi_{y1} - v_2 - \frac{h_2}{2}\phi_{y2}\right)}{\partial x}\bigg|_{x=0-} = \frac{\partial\left(v_1 - \frac{h_1}{2}\phi_{y1} - v_2 - \frac{h_2}{2}\phi_{y2}\right)}{\partial x}\bigg|_{x=0-} - \frac{\partial\left(v_1 - \frac{h_1}{2}\phi_{y1} - v_2 - \frac{h_2}{2}\phi_{y2}\right)}{\partial x}\bigg|_{x=0+} \tag{26}$$

Substituting the first equation in the constitutive law of Eq. (6) into Eqs. (25) and (26) and considering the global equilibrium conditions Eqs. (7)–(10), Eqs. (25) and (26) become:

$$\begin{aligned} &R_{11}N_{x10} + R_{12}N_{y10} + R_{16}N_{xy10} + Q_{11}M_{x10} + Q_{12}M_{y10} + Q_{16}M_{xy10} + R_{1T0} \\ &\quad = -(R_{11}(N_{x1} - N_{x10}) + R_{12}(N_{y1} - N_{y10}) + R_{16}(N_{xy1} - N_{xy10}) + Q_{11}(M_{x1} - M_{x10}) + Q_{12}(M_{y1} - M_{y10}) \\ &\qquad + Q_{16}(M_{xy1} - M_{xy10}) + R_{1T})|_{x=0} \end{aligned} \tag{27}$$

$$R_{16}N_{x10} + R_{26}N_{y10} + R_{66}N_{xy10} + Q_{16}M_{x10} + Q_{26}M_{y10} + Q_{66}M_{xy10} + R_{6T0}$$
$$= -(R_{16}(N_{x1} - N_{x10}) + R_{26}(N_{y1} - N_{y10}) + R_{66}(N_{xy1} - N_{xy10}) + Q_{16}(M_{x1} - M_{x10}) + Q_{26}(M_{y1} - M_{y10})$$
$$+ Q_{66}(M_{xy1} - M_{xy10}) + R_{6T})|_{x=0} \tag{28}$$

where the coefficients R_{ij} and Q_{ij} are given in Appendix A.

Recalling the global equilibrium conditions of Eqs. (7)–(10), we find that:

$$R_{1T0} = R_{1T}|_{x=0}, \qquad R_{6T0} = R_{6T}|_{x=0} \tag{29}$$

Noting the crack tip equilibrium conditions of Eqs. (11)–(15), we have

$$G_{\mathrm{II}} = \frac{1}{2}N_{xc}\left.\frac{\partial\left(u_1 - \frac{h_1}{2}\phi_{x1} - u_2 - \frac{h_2}{2}\phi_{x2}\right)}{\partial x}\right|_{x=0-} = \frac{1}{2}N_{xc}\left(\left(R_{11} - \frac{h_1}{2}Q_{11}\right)N_{xc} + \left(R_{16} - \frac{h_1}{2}Q_{16}\right)N_{xyc}\right)$$
$$= \frac{1}{2}(\delta_{11}N_{xc}^2 + \delta_{16}N_{xc}N_{xyc}) \tag{30}$$

$$G_{\mathrm{III}} = \frac{1}{2}N_{xyc}\left.\frac{\partial\left(v_1 - \frac{h_1}{2}\phi_{y1} - v_2 - \frac{h_2}{2}\phi_{y2}\right)}{\partial x}\right|_{x=0-} = \frac{1}{2}N_{xyc}\left(\left(R_{16} - \frac{h_1}{2}Q_{16}\right)N_{xc} + \left(R_{66} - \frac{h_1}{2}Q_{66}\right)N_{xyc}\right)$$
$$= \frac{1}{2}(\delta_{16}N_{xc}N_{xyc} + \delta_{66}N_{xyc}^2) \tag{31}$$

where three compliance coefficients are given by:

$$\delta_{11} = a_{11}^{(1)} + a_{11}^{(2)} - b_{11}^{(1)}h_1 + b_{11}^{(2)}h_2 + \frac{h_1^2}{4}d_{11}^{(1)} + \frac{h_2^2}{4}d_{11}^{(2)} \tag{32}$$

$$\delta_{16} = a_{16}^{(1)} + a_{16}^{(2)} - b_{16}^{(1)}h_1 + b_{16}^{(2)}h_2 + \frac{h_1^2}{4}d_{16}^{(1)} + \frac{h_2^2}{4}d_{16}^{(2)} \tag{33}$$

$$\delta_{66} = a_{66}^{(1)} + a_{66}^{(2)} - b_{66}^{(1)}h_1 + b_{66}^{(2)}h_2 + \frac{h_1^2}{4}d_{66}^{(1)} + \frac{h_2^2}{4}d_{66}^{(2)} \tag{34}$$

According to the second equation in the constitutive law of Eq. (6), we have

$$\left.\frac{\partial(w_1 - w_2)}{\partial x}\right|_{x=0-} = -(\phi_{x1} - \phi_{x2})|_{x=0-} + \left(a_{45}^{(1)} + a_{45}^{(2)}\right)Q_{y10} + \left(a_{55}^{(1)} + a_{55}^{(2)}\right)Q_{x10} \tag{35}$$

Note that

$$(\phi_{x1} - \phi_{x2})|_{x=0-} = (\phi_{x1} - \phi_{x2})|_{x=0+} = \left(a_{45}^{(1)} + a_{45}^{(2)}\right)Q_{y1}|_{x=0} + \left(a_{55}^{(1)} + a_{55}^{(2)}\right)Q_{x1}|_{x=0} \tag{36}$$

Considering the continuity of Q_{y1} across the delamination tip and combining Eqs. (35) and (36) with Eq. (13), we obtain:

$$G_{\mathrm{I}} = \frac{1}{2}\delta_Q Q_{xc}^2 \tag{37}$$

where δ_Q is the out-of-plane shear compliance coefficient of the two-plate system under in-plane open loading:

$$\delta_Q = \left(a_{55}^{(1)} + a_{55}^{(2)}\right) \tag{38}$$

Similarly, the total SERR at the crack tip can be written as:

$$G = \frac{1}{2}\left(\delta_{11}N_{xc}^2 + 2\delta_{16}N_{xc}N_{xyc} + \delta_{66}N_{xyc}^2 + \delta_Q Q_{xc}^2\right) \tag{39}$$

Eq. (39) indicates that no matter how many loadings are involved, the SERR can be expressed in terms of only three independent loading parameters N_{xc}, Q_{xc}, and N_{xyc}. Sankar and Sonik (1995) made a similar effort to express the SERR in terms of resultant force jumps at the crack tip where five forces (three concentrated forces and two concentrated moments) were used. Therefore, their expression is more complicated and makes the mode decomposition a very difficult task.

By computing the three concentrated crack tip forces N_{xc}, Q_{xc}, and N_{xyc}, the SERR can be simply evaluated as illustrated in Eq. (39). Revisiting Eqs. (27) and (28), we find that N_{xc} and N_{xyc} can be determined by:

$$\begin{pmatrix} N_{xc} \\ N_{xyc} \end{pmatrix} = \begin{pmatrix} R_{11} - \frac{h_1}{2}Q_{11} & R_{16} - \frac{h_1}{2}Q_{16} \\ R_{16} - \frac{h_1}{2}Q_{16} & R_{66} - \frac{h_1}{2}Q_{66} \end{pmatrix}^{-1} \times \begin{pmatrix} R_{11}N_{x10} + R_{12}N_{y10} + R_{16}N_{xy10} + Q_{11}M_{x10} + Q_{12}M_{y10} + Q_{16}M_{xy10} \\ R_{16}N_{x10} + R_{26}N_{y10} + R_{66}N_{xy10} + Q_{16}M_{x10} + Q_{26}M_{y10} + Q_{66}M_{xy10} \end{pmatrix} \tag{40}$$

while for determination of Q_{xc}, further analysis is needed, i.e., by solving a double plate system. For a simple 2-D problem, it can be analytically obtained as shown in Appendix B (see Eq. (B.26)).

2.3. Mode mix

It is a difficult but necessary task to extract mode mix of SERR in interface fracture mechanics due to its mode-mix-dependence. Two approaches of mode decomposition are commonly employed in the literature: the global approach based on the beam/plate theory and the local approach based on the local singular field close to the crack tip. There are conflicting experimental evidences in which approach is better to describe mixed mode fracture process. Tests on carbon/epoxy laminate composites showed that the global mode decomposition is more appropriate (Charalambides et al., 1992; Kinloch et al., 1993). On the other hand, the local approach was found to be well-adapted to analyze the bi-material interface fracture (Liechti and Chai, 1991; Akisanya and Fleck, 1992). To predict the delamination growth in unidirectional and multi-directional composites materials, Davidson et al. (2000a) found that the non-singular field (NSF) mode mix decomposition had the best accuracy. The NSF mode decomposition was developed by Davidson et al. (1997) based on the assumption that the parameters in plate theory could be best used to characterize mode mix. This method decomposed the mode mix in the same fashion as the local decomposition, however, with a different value of mode mix parameter Ω obtained by the experiments. In this study, both the global and local approaches are considered and explored.

As aforementioned, three separated modes of the SERR are already written in Eqs. (30), (31) and (37), and therefore, these three equations provide the partition method in a general 3-D case. It has been recently shown by Wang (2003) that the SERR expressions in Eqs. (30), (31) and (37) are in a limit situation for a cohesive fracture of two plates bonded by a "thin" layer of adhesive as the thickness of adhesive layer approaches to infinitesimal. Therefore, this mode decomposition simulates the presence of a perceived thin adhesive resin layer embedding in the laminas. This decomposition is called "global decomposition" in this paper since only the plate theory is used and the local oscillatory stress and displacement fields are ignored (Wang, 2003). However, this global method is different from the global mode mix decomposition method by Williams (1988) and the non-smooth model by Point and Sacco (1996). Williams (1988) developed the global decomposition based on classical beam theory and three simple assumptions, which were only reasonable for the symmetric delamination. As a result, Williams' method provided roughly the approximate solutions (Suo and Hutchinson, 1990; Davidson et al., 1995) and there was no obvious physical meaning of the method for

asymmetric delamination. On the other hand, the non-smooth model of Point and Sacco (1996) considered the fiber elongation along the interface, which was physically meaningful for asymmetric delamination; however, the difficulty still existed due to the presence of three crack tip forces (peel force V, shear force H and moment C in their notation) from the classical beam theory, and the concentrated moment C at the crack tip could contribute to all the fracture modes. Therefore, the error could be introduced by their assumption on the contribution of C to the fracture mode. While in the present method, there is no concentrated moment at the crack tip, which therefore makes the mode decomposition very straightforward. Point and Sacco (1996) also proposed a regularized laminate model which presented the SERRs of mode I and II as a function of interface property since a linear elastic interface model was used. Their approach was improved by Bruno and Greco (2001), in which the transverse shear deformation was incorporated.

This study presents a closed-form solution of the limit situation when the interface layer is infinitesimal in a 3-D extension. In the present global method, the first-order shear deformable plate kinematics is employed, and the actual displacement at the crack tip is much more complicated. Therefore, the accuracy of the present model depends on the accuracy of simulating delamination configuration by the plate model. For most beam type fracture specimens, such as double cantilever beam (DCB), end-notched flexure (ENF), and mixed mode bending (MMB) specimens, when the crack length is sufficiently long, this model can provide excellent results. The accuracy can be further enhanced by a more refined plate theory or multilayer plate formulation (Zou et al., 2001).

The strain energy release rate can be related to the modulus of stress intensity factor (Yang et al., 2000) as:

$$G = \frac{1}{4}\left[\frac{d_{22}}{\cosh^2 \pi\varepsilon}K_{\mathrm{I}}^2 + \left(d_{11} - \frac{w_{21}^2}{d_{22}}\right)K_{\mathrm{II}}^2 + \left(d_{33} - \frac{w_{32}^2}{d_{22}}\right)K_{\mathrm{III}}^2 + 2\left(d_{13} + \frac{w_{21}w_{32}}{d_{22}}\right)K_{\mathrm{II}}K_{\mathrm{III}}\right] \tag{41}$$

where d_{11}, d_{22}, d_{33}, d_{13}, w_{21} and w_{32} are the elements of bi-material matrix (Hwu, 1993). From linearity consideration, the stress intensity factors can be determined by the crack tip force as:

$$\begin{pmatrix} K_{\mathrm{I}} \\ K_{\mathrm{II}} \\ K_{\mathrm{III}} \end{pmatrix} = \begin{pmatrix} k_{11} & k_{12} & k_{13} \\ k_{21} & k_{22} & k_{23} \\ k_{31} & k_{32} & k_{33} \end{pmatrix} \begin{pmatrix} Q_{xc} \\ N_{xc} \\ N_{xyc} \end{pmatrix} \tag{42}$$

where k_{ij} are the coefficients need to be determined. Substituting Eq. (42) into Eq. (41) and then comparing with Eq. (40), six coefficients of k_{ij} in terms of the remaining three can be obtained. Finite element method is generally used to determine the remaining coefficients (Davidson et al., 1995; Yang et al., 2000).

3. Application: modified 2-D crack tip element

As an application example of the present method, a plane strain delamination problem of Fig. 4 is analyzed, in which the SERR and SIF have been expressed in terms of concentrated force N_c and moment M_c at the crack tip (the same notation given in Davidson et al., 1995). Essentially the same results have also

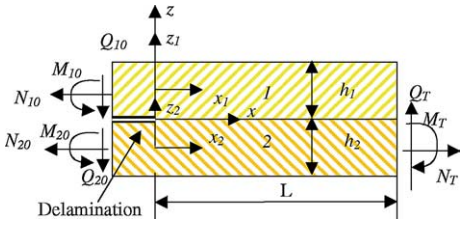

Fig. 4. 2-D crack tip element.

been given by Sheinman and Kardomateas (1997), but in the same style as in Suo and Hutchinson (1990). Both of these two solutions are based on the classical plate theory, and therefore, the transverse shear deformation is not accounted for. As shown in the study of Bruno and Greco (2001), the transverse shear plays a significant role in the SERR and therefore is considered in this study (Fig. 4).

3.1. Strain energy release rate

The normal concentrated force at the crack tip in Eq. (40) can be simplified as:

$$N_{xc} = \frac{2(Q_{11}M + R_{11}N)}{h_1 Q_{11} - 2R_{11}} \tag{43}$$

The transverse (peeling) concentrated force is solved (see Appendix B) as:

$$Q_{xc} = -Q - k\left(M + \frac{h_1 N}{2}\right) \tag{44}$$

where M, N and Q are defined in Eq. (B.27). Therefore, the SERRs can be written in the individual mode of global sense as:

$$G_{\mathrm{I}} = \frac{1}{2}\delta_{11}N_{xc}^2 = \frac{(Q_{11}M + R_{11}N)^2}{h_1 Q_{11} - 2R_{11}} \tag{45}$$

$$G_{\mathrm{II}} = \frac{1}{2}\delta_Q Q_{xc}^2 = \frac{\delta_Q}{2}\left(Q + k\left(M + \frac{h_1 N}{2}\right)\right)^2 \tag{46}$$

and,

$$G = \frac{1}{2}\delta_{11}N_{xc}^2 + \frac{1}{2}\delta_Q Q_{xc}^2 = \frac{1}{2}\left(C_N N^2 + C_Q Q^2 + C_M M^2 + C_{MN} MN + C_{NQ} NQ + C_{MQ} MQ\right) \tag{47}$$

where,

$$C_N = a_{11}^{(1)} + a_{11}^{(2)} + (h_1 + h_2)b_{11}^{(2)} + \frac{(h_1 + h_2)^2 d_{11}^{(2)}}{4}, \qquad C_Q = h_{55}^{(1)} + h_{55}^{(2)}, \qquad C_M = d_{11}^{(1)} + d_{11}^{(2)}$$

$$C_{MN} = 2\left(b_{11}^{(1)} + b_{11}^{(2)}\right) + (h_1 + h_2)d_{11}^{(2)}, \qquad C_{NQ} = \left(h_{55}^{(1)} + h_{55}^{(2)}\right)kh_1, \qquad C_{MQ} = 2\left(h_{55}^{(1)} + h_{55}^{(2)}\right)k$$

The expression of SERR in Eq. (47) is the same as the one obtained by Schapery and Davidson (1990) and Sheinman and Kardomateas (1997), except that three new terms associated with Q, which indicate the contribution of transverse shear to the total SERR, are introduced. In Eq. (47), $C_Q Q^2/2$ is due to the transverse shear deformation in the cracked region; while $C_{NQ}NQ/2$ and $C_{MQ}MQ/2$ arise from the transverse shear deformation in the uncracked region. The closed-form solutions obtained by Bruno and Greco (2001) for geometrically symmetric plates can be easily derived using the present formula of Eq. (47) by substituting the specific loading and laminate properties.

3.2. Mode decomposition and stress intensity factor

The global decomposition of mode mix is given in Eqs. (45) and (46). In this section, the local decomposition of fracture mode is studied. Following the same approach as in Sheinman and Kardomateas (1997), the top and bottom sub-laminates are replaced by equivalent orthotropic plates with their principle material axes aligned with the reference coordinate axes.

The strain energy release rate can be related to the modulus of stress intensity factor (Suo, 1990) as:

$$G = \frac{H_{11}}{4\cosh^2(\pi\varepsilon)}|K|^2 \tag{48}$$

where

$$\varepsilon = \frac{1}{2\pi}\ln\left(\frac{1-\beta}{1+\beta}\right) \tag{49}$$

$$\beta = \left([\sqrt{s_{11}s_{33}}+s_{13}]_2 - [\sqrt{s_{11}s_{33}}+s_{13}]_1\right)\Big/\sqrt{H_{11}H_{33}} \tag{50}$$

$$H_{11} = \left[2n\lambda^{\frac{1}{4}}\sqrt{s_{11}s_{33}}\right]_1 + \left[2n\lambda^{\frac{1}{4}}\sqrt{s_{11}s_{33}}\right]_2 \tag{51}$$

and

$$H_{33} = \left[2n\lambda^{-\frac{1}{4}}\sqrt{s_{11}s_{33}}\right]_1 + \left[2n\lambda^{-\frac{1}{4}}\sqrt{s_{11}s_{33}}\right]_2 \tag{52}$$

Here β is the generalization of one of Dundurs' (1969) parameters for isotropic materials and ε is the biomaterial constant. The subscripts "1" and "2" used outside the square brackets in the above expressions refer to the materials of top and bottom plates, respectively. The non-dimensional parameters λ and n are given by:

$$\lambda = \frac{s_{11}}{s_{33}}, \qquad n = \sqrt{\frac{1}{2}(1+\rho)} \tag{53}$$

where

$$\rho = \frac{1}{2}\frac{2s_{13}+s_{33}}{\sqrt{s_{11}s_{33}}} \tag{54}$$

s_{ij} are the material compliance coefficients and defined in the conventional fashion.

By comparing Eqs. (47) and (48), the magnitude of complex stress intensity factor is obtained as:

$$|K|^2 = \frac{p^2}{2}\left(\delta_{11}N_{xc}^2 + \delta_Q Q_{xc}^2\right) \tag{55}$$

where

$$p = \frac{2\cosh(\pi\varepsilon)}{\sqrt{H_{11}}} \tag{56}$$

Based on the dimensional consideration and linearity, the complex stress intensity factor K can be written in the form

$$K = \left(a\sqrt{\delta_Q}Q_{xc} + b\sqrt{\delta_{11}}N_{xc}\right)\frac{p}{\sqrt{2}}h_1^{-i\varepsilon} \tag{57}$$

where a and b are the dimensionless complex numbers which only depend on the geometric parameters and Dundurs's parameters.

Substituting Eq. (57) into Eq. (55) and comparing corresponding terms give

$$a\bar{a} = 1, \qquad b\bar{b} = 1, \qquad a\bar{b} + \bar{a}b = 0 \tag{58}$$

Let

$$a = e^{i\omega_1} \tag{59}$$

then:

$$b = ie^{i\omega_1} \tag{60}$$

and Eq. (57) can be re-written as:

$$K = K_G h_1^{-i\varepsilon} e^{i\omega_1} \tag{61}$$

where, ω_1 is an unknown parameter and needs to be determined; and

$$K_G = \frac{p}{\sqrt{2}}\left(\sqrt{\delta_Q}Q_{xc} + i\sqrt{\delta_{11}}N_{xc}\right) = |K_G|e^{i\psi_G} \tag{62}$$

Obviously, K_G is the complex stress intensity factor based on the global SERR partition of Eqs. (45) and (46); ψ_G is the loading phase angle of global decomposition and given as:

$$\psi_G = \arctan\left(\frac{\sqrt{\delta_{11}}N_{xc}}{\sqrt{\delta_Q}Q_{xc}}\right) = \arctan\left(\sqrt{\frac{G_{II}}{G_I}}\right) \tag{63}$$

Suo and Hutchinson (1990) obtained a mode mix parameter ω, which is defined differently, by solving an integral equation. Davidson et al. (1995) used the finite element analysis to obtain the mode mix parameter Ω and provided an equation to relate ω and Ω. To make use of their solution, we revisit Eq. (47) and rewrite Eq. (55) as:

$$|K|^2 = \frac{p^2}{2}\left(C_N N^2 + C_M M^2 + C_Q Q^2 + C_{MN} MN + C_{NQ} NQ + C_{MQ} MQ\right) \tag{64}$$

Following the similar procedure described above, we can write the stress intensity factor K as:

$$K = K_1 + iK_2 = \left(\sqrt{C_N}N - ie^{i\gamma_1}\sqrt{C_M}M - ie^{i\gamma_2}\sqrt{C_Q}Q\right)\frac{p}{\sqrt{2}}h_1^{-i\varepsilon}e^{i\omega} \tag{65}$$

where ω is defined in the same way as in Suo and Hutchinson (1990) and

$$\sin(\gamma_1) = \frac{C_{MN}}{2\sqrt{C_M C_N}}, \qquad \sin(\gamma_2) = \frac{C_{NQ}}{2\sqrt{C_N C_Q}} \tag{66}$$

By comparing Eqs. (61) and (65), we obtain:

$$\omega_1 = \omega + \gamma_2 - \frac{\pi}{2} \tag{67}$$

It is convenient to use the combination $Kh_1^{i\varepsilon}$ as suggested by Rice (1988) and define:

$$Kh_1^{i\varepsilon} = |K|e^{i\psi} = K_I + iK_{II} = K_G e^{i\omega_1} = |K_G|e^{i(\omega_1+\psi_G)} \tag{68}$$

Then the individual stress intensity factors are given by:

$$K_I = |K_G|\cos(\psi_G + \omega_1) = \frac{p}{\sqrt{2}}\left(\sqrt{\delta_N}N_{xc}\cos(\omega_1) - \sqrt{\delta_Q}Q_{xc}\sin(\omega_1)\right) \tag{69}$$

$$K_{II} = |K_G|\sin(\psi_G + \omega_1) = \frac{p}{\sqrt{2}}\left(\sqrt{\delta_N}N_{xc}\sin(\omega_1) + \sqrt{\delta_Q}Q_{xc}\cos(\omega_1)\right) \tag{70}$$

The phase angle ψ defined in Eq. (68) is given by:

$$\psi = \psi_G + \omega_1 = \tan^{-1}\left(\frac{\sqrt{\delta_N}N_{xc}\sin(\omega_1) + \sqrt{\delta_Q}Q_{xc}\cos(\omega_1)}{\sqrt{\delta_N}N_{xc}\cos(\omega_1) - \sqrt{\delta_Q}Q_{xc}\sin(\omega_1)}\right) \tag{71}$$

or in the fashion of Suo and Hutchinson (1990) as:

$$K_{\mathrm{I}} = \frac{p}{\sqrt{2}}\left(\sqrt{C_N}N\cos(\omega) + \sqrt{C_M}M\sin(\omega+\gamma_1) + \sqrt{C_Q}Q\sin(\omega+\gamma_2)\right) \tag{72}$$

$$K_{\mathrm{II}} = \frac{p}{\sqrt{2}}\left(\sqrt{C_N}N\sin(\omega) - \sqrt{C_M}M\cos(\omega+\gamma_1) - \sqrt{C_Q}Q\cos(\omega+\gamma_2)\right) \tag{73}$$

$$\psi = \tan^{-1}\left(\frac{\sqrt{C_N}N\sin(\omega) - \sqrt{C_M}M\cos(\omega+\gamma_1) - \sqrt{C_Q}Q\cos(\omega+\gamma_2)}{\sqrt{C_N}N\cos(\omega) + \sqrt{C_M}M\sin(\omega+\gamma_1) + \sqrt{C_Q}Q\sin(\omega+\gamma_2)}\right) \tag{74}$$

Recalling Eq. (47), the associated mode I and II SERRs are defined following the procedures in Davidson et al. (1995) as

$$G_{\mathrm{I}}^{*} = \frac{1}{2}\left(\sqrt{C_N}N\cos(\omega) + \sqrt{C_M}M\sin(\omega+\gamma_1) + \sqrt{C_Q}Q\sin(\omega+\gamma_2)\right)^2 \tag{75}$$

$$G_{\mathrm{II}}^{*} = \frac{1}{2}\left(\sqrt{C_N}N\sin(\omega) - \sqrt{C_M}M\cos(\omega+\gamma_1) - \sqrt{C_Q}Q\cos(\omega+\gamma_2)\right)^2 \tag{76}$$

It is important to see that Eqs. (72) and (73) can be reduced to the expressions given in Sheinman and Kardomateas (1997) if the transverse shear force Q is neglected. This indicates that the present solution is a modification and an improvement of results from the classical beam/plate theory and accounts for the transverse shear deformation in the closed-form solution. These expressions (Eqs. (75) and (76)) are not available in the literature to the authors' best knowledge.

3.3. Relationship between local and global decompositions

As shown in the previous section, the global and local approaches reach different results since the different displacement fields are used. It appears that there is an angle shift ω_1 between the local and global mode decompositions (see Eqs. (61) and (62)). In the global approach, the displacement field near the crack tip is described by the first-order shear deformable plate; while the actual displacement field near the crack tip is complicated and oscillatory. Therefore, the mode decomposition by the global approach is an approximate solution and should be used with cautions in practice. A better global decomposition can be achieved by using more complicated displacement fields, such as the refined plate model based on sublaminate concept proposed by Zou et al. (2001). However, the displacement field at the tip of an interface crack, which is inherently oscillatory, cannot be captured by the plate-type model due to its assumption used (e.g., Eqs. (1) and (3) in this study).

Despite its strong inaccuracies, the global mode decomposition is still widely used in the literature to retrieve the fracture parameters due to its simplicity and convenience to use. By neglecting the transverse shear terms in Eqs. (45) and (46), a global decomposition proposed by Bruno and Greco (2001) was obtained. Not surprisingly, they also reported a significant difference when comparing their solution with the local method. Compared with other available global decompositions aforementioned, the present solutions are advantageous in that it accounts for effect of transverse shear. The relationship between the global and local decompositions given by Eq. (68) provides an excellent tool to evaluate the error in the available plate-type models on mode decomposition. This error is reflected by a loading angle shift ω_1 which represents

both the geometry and material mismatches along the interface as shown in Eq. (67). According to Eqs. (67) and (68), the exactly same result of the local and global decompositions can be reached only when both the bottom and top plates are the same in material properties and geometries (i.e., thickness). In such a case, there is no stress oscillation along the interface, and both the local and global decompositions give the SERR components as:

$$G_{\mathrm{I}} = \frac{1}{2}\left(\sqrt{\frac{3}{7}C_N}N + \sqrt{C_M}M + \sqrt{C_Q}Q\right)^2 \tag{77}$$

$$G_{\mathrm{II}} = \frac{2}{7}C_N N^2 \tag{78}$$

It should be recognized that the loading angle shift ω_1 in this study and the mode mix parameter Ω defined by Davidson et al. (1995) are identical, and it can be achieved by requiring:

$$\gamma_2 = \widehat{\Gamma} - \Gamma \tag{79}$$

where $\widehat{\Gamma}$ and Γ are given as:

$$\sin\widehat{\Gamma} = \frac{\hat{c}_{12}}{\sqrt{\hat{c}_1\hat{c}_2}}, \qquad \sin\Gamma = \frac{c_{12}}{\sqrt{c_1 c_2}} \tag{80}$$

where the coefficients $\hat{c}_1$, $\hat{c}_2$, $\hat{c}_{12}$, c_1, c_2 and c_{12} are defined in Davidson et al. (1995). Comparing Eq. (A2) of Davidson et al. (1995) and Eq. (47) of this study, we have

$$\hat{c}_1 = C_N, \qquad \hat{c}_2 = C_M, \qquad \hat{c}_{12} = \frac{1}{2}C_{MN} \tag{81}$$

Eq. (A4) in Davidson et al. (1995) gives:

$$c_1 = C_N - \frac{h_1}{2}C_{MN} + \frac{h_1^2}{4}C_M, \qquad c_2 = C_M, \qquad c_{12} = \frac{1}{2}C_{MN} - \frac{h_1}{2}C_M \tag{82}$$

Therefore:

$$\begin{aligned}\sin(\widehat{\Gamma} - \Gamma) &= \sin\widehat{\Gamma}\cos\Gamma - \cos\widehat{\Gamma}\sin\Gamma = \frac{\hat{c}_{12}}{\sqrt{\hat{c}_1\hat{c}_2}}\sqrt{1 - \frac{c_{12}^2}{c_1 c_2}} - \frac{c_{12}}{\sqrt{c_1 c_2}}\sqrt{1 - \frac{\hat{c}_{12}^2}{\hat{c}_1\hat{c}_2}} \\ &= \frac{h_1}{2}\sqrt{\frac{C_N C_M - \frac{1}{4}C_{MN}^2}{C_N\left(C_N - \frac{h_1}{2}C_{MN} + \frac{1}{4}C_M\right)}} = \frac{h_1}{2}\sqrt{\frac{C_N C_M - \frac{1}{4}C_{MN}^2}{C_N\delta_{11}}}\end{aligned} \tag{83}$$

On the other hand, we can rewrite k given in Appendix B as:

$$k = \sqrt{\frac{C_N C_M - \frac{1}{4}C_{MN}^2}{\delta_{11}(h_{55}^{(1)} + h_{55}^{(2)})}} \tag{84}$$

Then Eq. (66) can be expressed as

$$\sin(\gamma_2) = \frac{C_{NQ}}{2\sqrt{C_N C_Q}} = \frac{(h_{55}^{(1)} + h_{55}^{(2)})h_1}{2\sqrt{C_N(h_{55}^{(1)} + h_{55}^{(2)})}}\sqrt{\frac{C_N C_M - \frac{1}{4}C_{MN}^2}{\delta_{11}(h_{55}^{(1)} + h_{55}^{(2)})}} = \frac{h_1}{2}\sqrt{\frac{C_N C_M - \frac{1}{4}C_{MN}^2}{C_N\delta_{11}}} \tag{85}$$

Therefore, Eq. (79) is verified by comparing Eq. (85) of this study with Eq. (82) of Davidson et al. (1995).

3.4. Numerical example

As a numerical example and verification of the present study, an asymmetric double cantilever beam (ADCB) specimen is analyzed. The ADCB specimen (Xiao et al., 1993) was used to evaluate the fracture toughness of polymer/polymer and polymer/non-polymer bi-material interfaces (Fig. 5). For the ADCB specimen, the loading parameters N, M and Q can be easily determined as:

$$N = 0, \qquad M = -Pa, \qquad Q = -P \tag{86}$$

In the practical testing, the displacement control is often used in order to keep crack propagation stable. If the classical beam model is used, the resulting SERR based on the crack tip element method (Davidson et al., 1995) is obtained as:

$$G = \frac{3\Delta^2 E_1 E_2 h_1^3 h_2^3}{8a^4(E_1 h_1^3 + E_2 h_2^3)} \tag{87}$$

The loading phase angle is given as:

$$\psi = -\tan^{-1}\left(\frac{\cos(\omega+\gamma_1)}{\sin(\omega+\gamma_1)}\right) \tag{88}$$

While by the present method where the effect of transverse shear deformation is included, the resulting SERR is obtained as (Wang, 2003):

$$G = \frac{\left(\frac{1}{2}\delta_Q(1+ka)^2 + 2\delta_N\xi^2\frac{a^2}{(h_1\xi+2\eta)^2}\right)\Delta^2}{\frac{a^3}{3}\left(\frac{1}{D_1}+\frac{1}{D_2}\right)+\left(\frac{1}{B_1}+\frac{1}{B_2}\right)a - k\left(\frac{1}{B_1}+\frac{1}{B_2}\right)a^2} \tag{89}$$

and the loading phase angle is calculated by:

$$\psi = -\tan^{-1}\left(\frac{\sqrt{C_M}a\cos(\omega+\gamma_1)+\sqrt{C_Q}\cos(\omega+\gamma_2)}{\sqrt{C_M}a\sin(\omega+\gamma_1)+\sqrt{C_Q}\sin(\omega+\gamma_2)}\right) \tag{90}$$

The SERR and loading phase angle obtained by the classical CTE method and the present method are compared with the numerical solution of ADCB specimen by Xiao et al. (1993), of which the boundary element method (BEM) was applied. By comparing with existing closed-form solution, the accuracy of BEM predictions (within 3% difference) was examined by Xiao et al. (1993). In this study, the results by

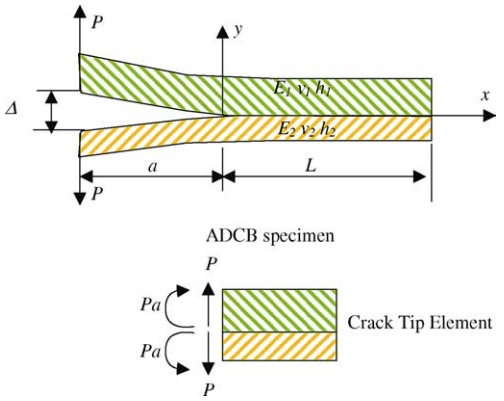

Fig. 5. Asymmetric double cantilever beam specimen.

BEM are used as the baseline data and regarded as accurate ones. For simplicity, the material of the specimen is chosen as homogeneous and isotropic.

The comparison of the SERR for an ADCB specimen between the present study which includes the effect of the transverse shear deformation and CTE analysis (Davidson and Sundararaman, 1996) which was primarily based on the classical beam theory is shown in Fig. 6. The SERR values in Fig. 6 are normalized by the BEM analysis results. As observed in Fig. 6, a significant improvement in accuracy of evaluating SERR is achieved by the present method. The CTE analysis ignores the transverse shear deformation and therefore over-evaluates the stiffness of the specimen and the total SERR in term of displacement Δ. The differences of the phase angles ψ of the ADCB specimen calculated by the CTE analysis and the present study from the BEM are compared in Fig. 7. It is observed that compared to the CTE analysis, the phase angle by the present study (Eq. (90)) is much closer to the BEM analysis data. The CTE seems to over-estimate the phase angle of the mode mix (if the sign of the phase angle is ignored), although the difference from the BEM analysis is not significant. It can be concluded that the shear deformation reduces the phase

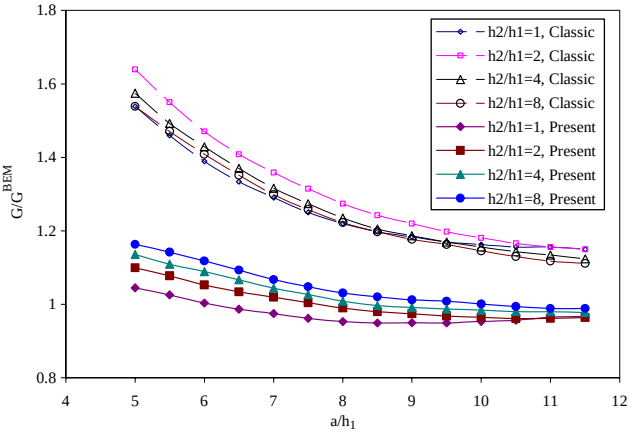

Fig. 6. Comparisons of SERR.

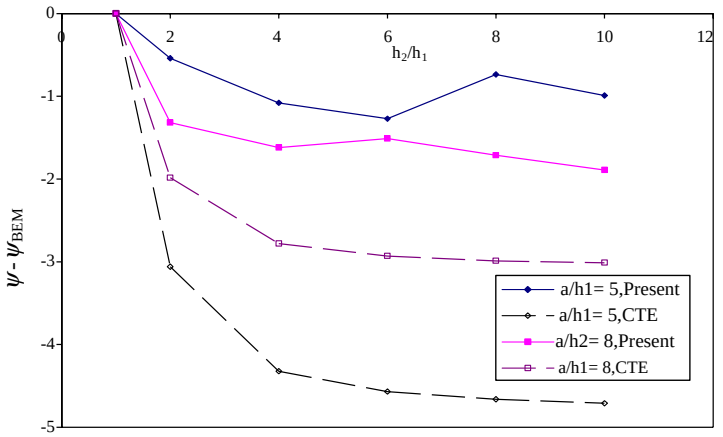

Fig. 7. Comparisons of load phase angle.

angle a little bit and the accuracy of the phase angle provided by the present study Eq. (90) is enhanced when compared to the CTE analysis.

As a matter of fact, the classical plate theory-based approach for interface fracture analysis is not appropriate when the slenderness ratio is small since the shear deformation effect is more pronounced in the specimen with moderate thickness and should not be ignored. By considering the effect of shear deformation, the present prediction of the SERR has improved the accuracy when compared to the conventional approach based on the classical plate theory. It can further imply that the shear deformation effect is significant in the interface fracture analysis, especially for the specimens with low transverse shear modulus and moderate thickness.

4. Conclusions

By modeling the delaminated composite plate as two Mindlin–Reissner sub-laminates on either side of the delamination plane, an explicit and more accurate solution of the SERR is obtained in this paper. The formulated SERR has shown to be determined by only three independent loading parameters, N_{xc}, Q_{xc} and N_{xyc} and as a result, the SIF is retrieved simply with the aid of two supplementary continuum analyses under arbitrary loading configurations. By simplifying the present 3-D solution to a plane strain delamination problem, the improved close-formed solutions of concentrated forces at the crack tip are analytically developed. The resulting SERRs and SIFs in the 2-D plane strain condition are reduced to the available classical plate theory-based solutions if the transverse shear is neglected. The relationship between the global and local mode mix decompositions is established, and the derived expressions of SERRs are for the first time available in the literature to "explicitly" include the effect of transverse shear in interface fracture analysis. A close agreement of the present solutions with the available numerical data of boundary element method indicates the accuracy and improvement of proposed approach compared to the classical plate theory-based model. In summary, the explicit and close-formed solutions of the SERR, SIF and their corresponding global and local mode decompositions with consideration of transverse shear deformation are developed, and more accurate predictions are achieved, especially when the delaminated composite plates have a relatively low transverse shear modulus or moderate thickness.

Acknowledgements

This study was partially supported by the National Science Foundation (CMS-0002829 and EHR-0090472).

Appendix A. The coefficients R_{ij} and Q_{ij} in Eqs. (27) and (28)

$$R_{11} = a_{11}^{(1)} - \frac{h_1}{2} b_{11}^{(1)} + a_{11}^{(2)} + \frac{h_2}{2} b_{11}^{(2)} + \frac{h_1 + h_2}{2} b_{11}^{(2)} + \frac{h_2(h_1 + h_2)}{4} d_{11}^{(2)} \tag{A.1}$$

$$R_{12} = a_{12}^{(1)} - \frac{h_1}{2} b_{12}^{(1)} + a_{12}^{(2)} + \frac{h_2}{2} b_{12}^{(2)} + \frac{h_1 + h_2}{2} b_{12}^{(2)} + \frac{h_2(h_1 + h_2)}{4} d_{12}^{(2)} \tag{A.2}$$

$$R_{16} = a_{16}^{(1)} - \frac{h_1}{2} b_{16}^{(1)} + a_{16}^{(2)} + \frac{h_2}{2} b_{16}^{(2)} + \frac{h_1 + h_2}{2} b_{16}^{(2)} + \frac{h_2(h_1 + h_2)}{4} d_{16}^{(2)} \tag{A.3}$$

$$R_{26} = a_{26}^{(1)} - \frac{h_1}{2} b_{26}^{(1)} + a_{26}^{(2)} + \frac{h_2}{2} b_{26}^{(2)} + \frac{h_1 + h_2}{2} b_{26}^{(2)} + \frac{h_2(h_1 + h_2)}{4} d_{26}^{(2)} \tag{A.4}$$

$$R_{66} = a_{66}^{(1)} - \frac{h_1}{2} b_{66}^{(1)} + a_{66}^{(2)} + \frac{h_2}{2} b_{66}^{(2)} + \frac{h_1 + h_2}{2} b_{66}^{(2)} + \frac{h_2(h_1 + h_2)}{4} d_{66}^{(2)} \tag{A.5}$$

$$Q_{11} = b_{11}^{(1)} - \frac{h_1}{2} d_{11}^{(1)} + b_{11}^{(2)} + \frac{h_2}{2} d_{11}^{(2)} \tag{A.6}$$

$$Q_{12} = b_{12}^{(1)} - \frac{h_1}{2} d_{12}^{(1)} + b_{12}^{(2)} + \frac{h_2}{2} d_{12}^{(2)} \tag{A.7}$$

$$Q_{16} = b_{16}^{(1)} - \frac{h_1}{2} d_{16}^{(1)} + b_{16}^{(2)} + \frac{h_2}{2} d_{16}^{(2)} \tag{A.8}$$

$$Q_{26} = b_{26}^{(1)} - \frac{h_1}{2} d_{26}^{(1)} + b_{26}^{(2)} + \frac{h_2}{2} d_{26}^{(2)} \tag{A.9}$$

$$Q_{66} = b_{66}^{(1)} - \frac{h_1}{2} d_{66}^{(1)} + b_{66}^{(2)} + \frac{h_2}{2} d_{66}^{(2)} \tag{A.10}$$

$$\begin{aligned} R_{1T0} = {} & \left(a_{11}^{(2)} + \frac{h_2}{2} b_{11}^{(2)}\right)(N_{x10} + N_{x20}) + \left(a_{12}^{(2)} + \frac{h_2}{2} b_{12}^{(2)}\right)(N_{y10} + N_{y20}) + \left(a_{16}^{(2)} + \frac{h_2}{2} b_{16}^{(2)}\right)(N_{xy10} + N_{xy20}) \\ & + \left(b_{11}^{(2)} + \frac{h_2}{2} d_{11}^{(2)}\right)\left(M_{x10} + M_{x20} + \frac{h_1 + h_2}{2} N_{x10}\right) + \left(b_{12}^{(2)} + \frac{h_2}{2} d_{12}^{(2)}\right)\left(M_{y10} + M_{y20} + \frac{h_1 + h_2}{2} N_{y10}\right) \\ & + \left(b_{16}^{(2)} + \frac{h_2}{2} d_{16}^{(2)}\right)\left(M_{xy10} + M_{xy20} + \frac{h_1 + h_2}{2} N_{xy10}\right) \end{aligned} \tag{A.11}$$

$$\begin{aligned} R_{6T0} = {} & \left(a_{16}^{(2)} + \frac{h_2}{2} b_{16}^{(2)}\right)(N_{x10} + N_{x20}) + \left(a_{26}^{(2)} + \frac{h_2}{2} b_{26}^{(2)}\right)(N_{y10} + N_{y20}) + \left(a_{66}^{(2)} + \frac{h_2}{2} b_{66}^{(2)}\right)(N_{xy10} + N_{xy20}) \\ & + \left(b_{16}^{(2)} + \frac{h_2}{2} d_{16}^{(2)}\right)\left(M_{x10} + M_{x20} + \frac{h_1 + h_2}{2} N_{x10}\right) + \left(b_{26}^{(2)} + \frac{h_2}{2} d_{26}^{(2)}\right)\left(M_{y10} + M_{y20} + \frac{h_1 + h_2}{2} N_{y10}\right) \\ & + \left(b_{66}^{(2)} + \frac{h_2}{2} d_{66}^{(2)}\right)\left(M_{xy10} + M_{xy20} + \frac{h_1 + h_2}{2} N_{xy10}\right) \end{aligned} \tag{A.12}$$

$$\begin{aligned} R_{1T} = {} & \left(a_{11}^{(2)} + \frac{h_2}{2} b_{11}^{(2)}\right) N_{xT} + \left(a_{12}^{(2)} + \frac{h_2}{2} b_{12}^{(2)}\right)(N_{y10} + N_{y20}) + \left(a_{16}^{(2)} + \frac{h_2}{2} b_{16}^{(2)}\right) N_{xyT} + \left(b_{11}^{(2)} + \frac{h_2}{2} d_{11}^{(2)}\right) M_{xT} \\ & + \left(b_{12}^{(2)} + \frac{h_2}{2} d_{12}^{(2)}\right)\left(M_{y10} + M_{y20} + \frac{h_1 + h_2}{2} N_{y10}\right) + \left(b_{16}^{(2)} + \frac{h_2}{2} d_{16}^{(2)}\right) M_{xyT} \end{aligned} \tag{A.13}$$

$$\begin{aligned} R_{6T} = {} & \left(a_{16}^{(2)} + \frac{h_2}{2} b_{16}^{(2)}\right) N_{xT} + \left(a_{26}^{(2)} + \frac{h_2}{2} b_{26}^{(2)}\right)(N_{y10} + N_{y20}) + \left(a_{66}^{(2)} + \frac{h_2}{2} b_{66}^{(2)}\right) N_{xyT} + \left(b_{16}^{(2)} + \frac{h_2}{2} d_{16}^{(2)}\right) M_{xT} \\ & + \left(b_{26}^{(2)} + \frac{h_2}{2} d_{26}^{(2)}\right)\left(M_{y10} + M_{y20} + \frac{h_1 + h_2}{2} N_{y10}\right) + \left(b_{66}^{(2)} + \frac{h_2}{2} d_{66}^{(2)}\right) M_{xyT} \end{aligned} \tag{A.14}$$

Appendix B. Crack tip forces in 2-D crack tip element

According to Reissner–Mindlin plate theory, the plane strain deformations of a two-plate system are given as:

$$U_i(x,y) = u_i(x) + y\phi_i(x) \tag{B.1}$$

$$W_i(x,y) = w_i(x) \tag{B.2}$$

where the subscript $i = 1$ or 2 represents the plate 1 or 2 of Fig. 1, respectively.

The strains in these two plates are given as:

$$\varepsilon_i^0 = \frac{\mathrm{d}u_i}{\mathrm{d}x}, \qquad \kappa_i = \frac{\mathrm{d}\phi_i}{\mathrm{d}x}, \qquad \gamma_{xyi} = \phi_i + \frac{\mathrm{d}w_i}{\mathrm{d}x} \tag{B.3}$$

The constitutive equation of laminate is written in the conventional way as:

$$\begin{pmatrix} N_i \\ M_i \end{pmatrix} = \begin{pmatrix} A_{11}^{(i)} & B_{11}^{(i)} \\ B_{11}^{(i)} & D_{11}^{(i)} \end{pmatrix} \begin{pmatrix} \frac{\mathrm{d}u_i}{\mathrm{d}x} \\ \frac{\mathrm{d}\phi_i}{\mathrm{d}x} \end{pmatrix}, \qquad Q_i = H_{55}^{(i)} \left(\phi_i + \frac{\mathrm{d}w_i}{\mathrm{d}x} \right) \tag{B.4}$$

or

$$\begin{pmatrix} \frac{\mathrm{d}u_i}{\mathrm{d}x} \\ \frac{\mathrm{d}\phi_i}{\mathrm{d}x} \end{pmatrix} = \begin{pmatrix} a_{11}^{(i)} & b_{11}^{(i)} \\ b_{11}^{(i)} & d_{11}^{(i)} \end{pmatrix} \begin{pmatrix} N_i \\ M_i \end{pmatrix}, \qquad \phi_i + \frac{\mathrm{d}w_i}{\mathrm{d}x} = h_{55}^{(i)} Q_i \tag{B.5}$$

At the interface of the two-plate system, the displacement continuity requires:

$$u_1 - \frac{h_1}{2}\phi_1 = u_2 + \frac{h_2}{2}\phi_2 \tag{B.6}$$

$$w_1 = w_2 \tag{B.7}$$

Differentiating Eq. (B.6) once and substituting the first equation in Eq. (B.5) yields:

$$a_{11}^{(1)} N_1 + b_{11}^{(1)} M_1 - \frac{h_1}{2}\left(b_{11}^{(1)} N_1 + d_{11}^{(1)} M_1 \right) = a_{11}^{(2)} N_2 + b_{11}^{(2)} M_2 + \frac{h_2}{2}\left(b_{11}^{(2)} N_2 + d_{11}^{(2)} M_2 \right) \tag{B.8}$$

Considering the global equilibrium conditions in Fig. 8, we have

$$N_1 + N_2 = N_{10} + N_{20} = N_T \tag{B.9}$$

$$Q_1 + Q_2 = Q_T \tag{B.10}$$

$$M_1 + M_2 + N_1 \frac{h_1 + h_2}{2} = M_{10} + M_{20} + N_{10} \frac{h_1 + h_2}{2} + Q_T x = M_T \tag{B.11}$$

Substituting Eqs. (B.9) and (B.10) into Eq. (B.8) gives:

$$R_{11} N_1 + Q_{11} M_1 = b_N N_T + b_M M_T \tag{B.12}$$

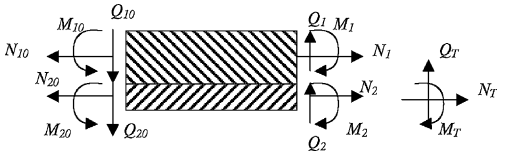

Fig. 8. Overall equilibrium of a two-plate system (plane-strain condition).

where

$$R_{11} = a_{11}^{(1)} + a_{11}^{(2)} - \frac{h_1 b_{11}^{(1)}}{2} + \frac{h_2 b_{11}^{(2)}}{2} + \frac{(h_1+h_2) b_{11}^{(2)}}{2} + \frac{h_2(h_1+h_2) d_{11}^{(2)}}{4},$$

$$Q_{11} = b_{11}^{(1)} + b_{11}^{(2)} - \frac{h_1 d_{11}^{(1)}}{2} + \frac{h_2 d_{11}^{(2)}}{2}, \qquad b_N = a_{11}^{(2)} + \frac{h_2 b_{11}^{(2)}}{2}, \qquad b_M = b_{11}^{(2)} + \frac{h_2 d_{11}^{(2)}}{2}$$

Differentiating Eq. (B.7) twice and considering Eq. (B.5) yields:

$$h_{55}^{(1)} \frac{\mathrm{d}Q_1}{\mathrm{d}x} - \frac{\mathrm{d}\phi_1}{\mathrm{d}x} = h_{55}^{(2)} \frac{\mathrm{d}Q_2}{\mathrm{d}x} - \frac{\mathrm{d}\phi_2}{\mathrm{d}x} \tag{B.13}$$

Substituting Eqs. (B.5) and (B.10) into Eq. (B.6), we obtain:

$$\left(h_{55}^{(1)} + h_{55}^{(2)}\right) \frac{\mathrm{d}Q_1}{\mathrm{d}x} = \left(b_{11}^{(1)} N_1 + d_{11}^{(1)} M_1\right) - \left(b_{11}^{(2)} N_2 + d_{11}^{(2)} M_2\right) \tag{B.14}$$

Considering the equilibrium condition of the plate 1, we have

$$Q_1 = \frac{\mathrm{d}M_1}{\mathrm{d}x} + \frac{h_1}{2} \frac{\mathrm{d}N_1}{\mathrm{d}x} \tag{B.15}$$

Combining Eq. (B.14) with Eqs. (B.9) and (B.11) results in:

$$\begin{aligned} &\left(h_{55}^{(1)} + h_{55}^{(2)}\right) \left(\frac{\mathrm{d}^2 M_1}{\mathrm{d}x^2} + \frac{h_1}{2} \frac{\mathrm{d}^2 N_1}{\mathrm{d}x^2} \right) \\ &\quad = \left(b_{11}^{(1)} + b_{11}^{(2)} + \frac{(h_1+h_2) d_{11}^{(2)}}{2} \right) N_1 + \left(d_{11}^{(1)} + d_{11}^{(2)} \right) M_1 - b_{11}^{(2)} N_T - d_{11}^{(2)} M_T \end{aligned} \tag{B.16}$$

By eliminating M_1 from Eq. (B.12), Eq. (B.16) becomes:

$$\begin{aligned} &\left(h_{55}^{(1)} + h_{55}^{(2)}\right) \left(-\frac{R_{11}}{Q_{11}} + \frac{h_1}{2} \right) \frac{\mathrm{d}^2 N_1}{\mathrm{d}x} \\ &\quad = \left(b_{11}^{(1)} + b_{11}^{(2)} + \frac{(h_1+h_2) d_{11}^{(2)}}{2} + \frac{(d_{11}^{(1)} + d_{11}^{(2)}) R_{11}}{Q_{11}} \right) N_1 \\ &\qquad - \left(d_{11}^{(1)} + d_{11}^{(2)} \right) \left(\frac{b_N}{R_{11}} N_T - \frac{b_M}{Q_{11}} M_T \right) - b_{11}^{(2)} N_T - d_{11}^{(2)} M_T \end{aligned} \tag{B.17}$$

Solving Eq. (B.17) gives the axial force of plate 1 as:

$$N_1 = c\mathrm{e}^{-kx} + N_{1C} \tag{B.18}$$

where

$$k^2 = \frac{b_{11}^{(1)} + b_{11}^{(2)} + \frac{(h_1+h_2) d_{11}^{(2)}}{2} - \frac{R_{11}}{Q_{11}} (d_{11}^{(1)} + d_{11}^{(2)})}{(h_{55}^{(1)} + h_{55}^{(2)}) \left(-\frac{R_{11}}{Q_{11}} + \frac{h_1}{2} \right)}$$

$$N_{1C} = \frac{(d_{11}^{(1)} + d_{11}^{(2)}) \left(\frac{b_N}{R_{11}} N_T - \frac{b_M}{Q_{11}} \right) - b_{11}^{(2)} N_T - d_{11}^{(2)} M_T}{b_{11}^{(1)} + b_{11}^{(2)} + \frac{(h_1+h_2) d_{11}^{(2)}}{2} - \frac{(d_{11}^{(1)} + d_{11}^{(2)}) R_{11}}{Q_{11}}}$$

Recalling Eqs. (B.12) and (B.15), M_1 and Q_1 can be obtained as:

$$M_1 = -\frac{R_{11}}{Q_{11}} c\mathrm{e}^{-kx} + M_{1C} \tag{B.19}$$

$$Q_1 = \left(\frac{R_{11}}{Q_{11}} - \frac{h_1}{2}\right) ck\mathrm{e}^{-kx} + Q_{1C} \tag{B.20}$$

where

$$M_{1C} = -\frac{R_{11}}{Q_{11}} N_{1C} + \frac{b_N}{Q_{11}} N_T + \frac{b_M}{Q_{11}} M_T$$

$$Q_{1C} = \frac{\mathrm{d}M_{1C}}{\mathrm{d}x} + \frac{h_1}{2}\frac{\mathrm{d}N_{1C}}{\mathrm{d}x}$$

Two concentrated forces N_{xc} and Q_{xc} are presented in the SERR expressions (see Eqs. (42) and (43)). Considering the equilibrium conditions at the crack tip (Fig. 9), we have

$$N_{10} = -N_{xc} + N_1(0) \tag{B.21}$$

$$M_{10} = \frac{h_1}{2} N_{xc} + M_1(0) \tag{B.22}$$

$$Q_{10} = -Q_{xc} + Q_1(0) \tag{B.23}$$

Integral coefficients c in Eq. (B.18) and two concentrated forces N_{xc} and Q_{xc} can be then obtained as:

$$c = \frac{(2M + h_1 N)Q_{11}}{h_1 Q_{11} - 2R_{11}} \tag{B.24}$$

$$N_{xc} = \frac{2(Q_{11}M + R_{11}N)}{h_1 Q_{11} - 2R_{11}} \tag{B.25}$$

$$Q_{xc} = -Q - k\left(M + \frac{h_1 N}{2}\right) \tag{B.26}$$

where

$$M = M_{10} - M_1(0), \qquad N = N_{10} - N_1(0), \qquad Q = Q_{10} - Q_1(0) \tag{B.27}$$

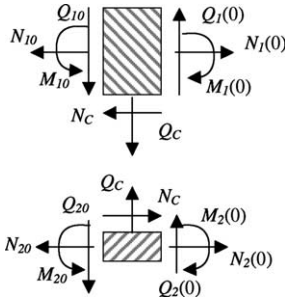

Fig. 9. Equilibrium at the crack tip.

References

Akisanya, A.R., Fleck, N.A., 1992. Brittle fracture of adhesive joints. International Journal of Fracture 59, 93–114.

Barbero, E.J., 1998. Introduction to Composite Materials Design. Taylor & Francis, Inc., Philadelphia, PA.

Beuth, J.L., 1996. Separation of crack extension modes in orthotropic delamination models. International Journal of Fracture 77, 305–321.

Bruno, D., Greco, F., 2001. Mixed mode delamination in plates: a refined approach. International Journal of Solids and Structures 38, 9149–9177.

Charalambides, M., Kinloch, A.J., Wang, Y., Williams, J.G., 1992. On the analysis of mixed-mode failure. International Journal of Fracture 54, 269–291.

Chatterjee, S.N., Ramnath, V., 1988. Modeling laminate composite structures as assemblage of sublaminates. International Journal of Solids and Structures 24, 439–458.

Davidson, B.D., Sundararaman, V., 1996. A single leg bending test for interfacial fracture toughness determination. International Journal of Fracture 78, 193–210.

Davidson, B.D., Hu, H., Schapery, R.A., 1995. An analytical crack-tip element for layered elastic structures. Journal of Applied Mechanics 62, 294–305.

Davidson, B.D., Fariello, P.L., Hudson, R.C., Sundararaman, V., 1997. Accuracy assessment of the singular field-based mode mix decomposition procedure for the prediction of delamination. In: Hooper, S.J. (Ed.), Composite Materials: Testing and Design. In: ASTM STP 1242, vol. 13. American Society for Testing and Materials, pp. 109–128.

Davidson, B.D., Gharibian, S.J., Yu, L.J., 2000a. Evaluation of energy release rate-based approaches for predicting delamination growth in laminated composites. International Journal of Fracture 105, 343–365.

Davidson, B.D., Yu, L.J., Hu, H., 2000b. Determination of energy release rate and mode mix in three-dimensional layered structures using plate theory. International Journal of Fracture 105, 81–104.

Dundurs, J., 1969. Mathematical theory of dislocations. ASME Journal of Applied Mechanics 36, 650–652.

Hu, H., 1995. Analytical determination of energy release rate and mode mix for interfacial cracks. Ph.D. Dissertation, Department of Mechanical, Aerospace and Manufacturing Engineering, Syracuse University, Syracuse, NY, USA.

Hwu, C., 1993. Fracture parameters for the orthotropic bimaterial interface cracks. Engineering Fracture Mechanics 45, 89–97.

Kinloch, A.G., Wang, Y., Williams, J.G., Yayal, P., 1993. The mixed mode delamination of fiber composite materials. Composite Science Technology 47, 225–237.

Liechti, K.M., Chai, Y.S., 1991. Biaxial loading experiments for determining interfacial fracture toughness. Journal of Applied Mechanics 58, 680–687.

Matos, P.P.L., McMeeking, R.M., Charalambides, P.G., Drory, M.D., 1989. A method for calculating stress intensities in bimaterial fracture. International Journal of Fracture 40, 235–254.

Nillsson, K.-F., Asp, L.E., Alpman, J.E., Nystdt, L., 2001. Delamination buckling and growth for delaminations at different depths in a slender composite panel. International Journal of Solids and Structures 38, 3039–3071.

O'Brien, T.K., 1982. Characterization of delamination onset and growth in a composite laminate. In: Reifsnider, K.L. (Ed.), Damage in Composite Materials. In: ASTM STP 775. ASTM, pp. 140–147.

O'Brien, T.K., 1990. Towards a damage tolerance philosophy for composite materials and structures. In: Garbo, S.P. (Ed.), Composite Materials: Testing and Design. In: ASTM STP 1059, vol. 9. ASTM, pp. 7–33.

Park, O., Sanker, B.V., 2002. Crack-tip force method for computing energy release rate in delaminated plates. Composite Structures 55, 429–434.

Point, N., Sacco, E., 1996. Delamination of beams: an application to the DCB specimen. International Journal of Fracture 79, 225–247.

Qian, W., Sun, C.T., 1998. Methods for calculation of stress intensity factors for interfacial cracks between two orthotropic solids. International Journal of Solids and Structures 35, 3317–3330.

Rice, J.R., 1988. Elastic fracture mechanics concepts for interfacial cracks. Journal of Applied Mechanics 55, 98–103.

Sankar, B.V., Sonik, V., 1995. Pointwise engergy release rate in delaminated plates. AIAA Journal 33, 1312–1318.

Schapery, R.A., Davidson, B.D., 1990. Prediction of energy release rate for mixed-mode delamination using classical plate theory. Applied Mechanics Review 43, S281–S287.

Sheinman, I., Kardomateas, G.K., 1997. Energy release rate and stress intensity factors for delaminated composite laminates. International Journal of Solids and Structures 34, 451–459.

Sun, C.T., Qian, W., 1997. The use of finite extension strain energy release rates in fracture of interface crack. International Journal of Solids and Structures 34, 2595–2609.

Suo, Z., 1990. Singularities, interfaces and cracks in dissimilar anisotropic media. Proceedings of the Royal Society of London, Series A—Mathematical Physical and Engineering Sciences 427, 331–358.

Suo, Z., Hutchinson, J.W., 1990. Interface crack between two elastic layers. International Journal of Fracture 43, 1–18.

Venkatesha, K.S., Ramamurthy, T.S., Dattagura, B., 1996. Generalized modified crack closure integral and its application to interface crack problems. Computers and Structures 60 (4), 665–676.

Wang, S.S., 1982. Fracture mechanics for delamination problems in composite materials. In: Hayashi, T., Kawata, K., Umekawa, S. (Eds.), Progress in Science and Engineering of Composites. Proceedings ICCM-IV, Tokyo, pp. 287–296.

Wang, J.L., 2003. Mechanics and fracture of hybrid material interface bond. Ph.D. Dissertation, Department of Civil Engineering, The University of Akron, Akron, OH, USA.

Wang, A.S.D., Crossman, F.W., 1980. Initiation and growth of transverse cracks and edge delamination in composites, Parts 1 and 2. Journal of Composite Materials (Supl.), 71–106.

Williams, J.G., 1988. On the calculation of energy release rate for cracked laminates. International Journal of Fracture 36, 101–119.

Xiao, F., Hui, C.Y., Kramer, E.J., 1993. Analysis of a mixed mode fracture specimen: the asymmetric double cantilever beam. Journal of Material Science 28 (20), 5620–5629.

Yang, Z., Sun, C.T., Wang, J., 2000. Fracture mode separation for delamination in plate-like composite structures. AIAA Journal 38, 868–874.

Zou, Z., Reid, S.R., Soden, P.D., Li, S., 2001. Mode separation of energy release rate for delamination in composite laminates using sublaminates. International Journal of Solids and Structures 38 (15), 2597–2613.